Extraction of Underwater Laver Cultivation Area by SAR Polarimetric Entropy

#E.S. Won[1], and K. Ouchi[1]

[1] Department of Computer Science, National Defense Academy
1-10-20, Hashirimizu, Yokosuka, Kanagawa, 239-8686 Japan.
email: en49057@nda.ac.jp, ouchi@nda.ac.jp

In January 2006, Advanced Land Observing Satellite (ALOS) was launched by Japan Aerospace Exploration Agency (JAXA), carrying Phased Array L-band Synthetic Aperture Radar (PALSAR). Although ALOS-PALSAR is aimed mainly on land observation, it can play a major role in the field of oceanography such as ocean surveillance, maritime meteorology and pollution. Especially, using polarimetric data of ALOS-PALSAR, it can obtain more information than single-polarization data. Thus, radar remote sensing using polarimetric information comes to the forefront of the current research.

This paper describes a technique of extracting underwater laver cultivation nets by using entropy analysis from ALOS-PALSAR polarimetric data in the water around the Futtsu Horn, Chiba, Japan. The method is based on the difference in the backscattered fields from the almost specular surface above the laver nets and slightly rough surface in open water. Under weak to moderate wind conditions, the backscattered field from open water is dominated by the surface (Bragg) scattering. While the laver nets are placed at a few centimeters below the sea surface, so that waves are damped, resulting in the specular surface causing little radar backscatter. This difference in radar cross section (RCS) can be detected by X-band TerraSAR-X, but the difference is too small to detect by PALSAR because both the surfaces are effectively smooth for L-band microwave. However, since the radar backscatter from the specular surface is at the system noise level, the image can be considered as arising from a random process of various scattering contributions. The polarimetric entropy should then be higher than the single-bounce surface scattering from the open water. We will show, in this paper, that the polarimetric entropy is an effective means of identifying the underwater laver nets compared with the RCS-based method from PALSAR L-band data.

1 Test site and meteorological data

In this paper, we report the preliminary results on the study of extracting underwater laver cultivation areas using polarimetric PALSAR data over the Futtsu Horn, Japan. The laver cultivation in this water, is maintained from October to April, using underwater nets of each size approximately 123×8.3 m, and a single net consists of 12 smaller nets of size 18×1.5 m (there are some gaps among the combined nets). The data we used in the experiments are the ALOS-PALSAR PLR 21.5 data (PoLaRimetric data at off-nadir angle 21.5° acquired on 24th November and TerraSAR-X data of 26th December, 2008. The wave data were from the Nationwide Ocean Wave information network for Port and HArbourS (NOWPHAS) data acquired at a station located at approximately 7 km west from the cultivation area [1]. The wind data were measured at a station close to the experimental site, and were supplied by the Japan Weather Association (JWA). The data acquisition times varied depending on the dates, but were centered at 13:30±10 min. (Universal Time) corresponding to 10:30 pm at local time. These data show that the sea was calm (significant waveheight 0.6 m and 0.6 m, wind speed 2.0 m/s and 5.8 m/s for PALSAR and TerraSAR-X acquisition times respectively) at these times.

2 Analysis of PALSAR and TerraSAR-X amplitude data

Fig.1 shows the ALOS-PALSAR amplitude image (HH polarization) on the left and on the right the TerraSAR-X amplitude image (HH polarization) of the laver cultivation area. The image size is approximately 3.3 km and 4.6 km in azimuth and range directions respectively. The dark areas are the sea

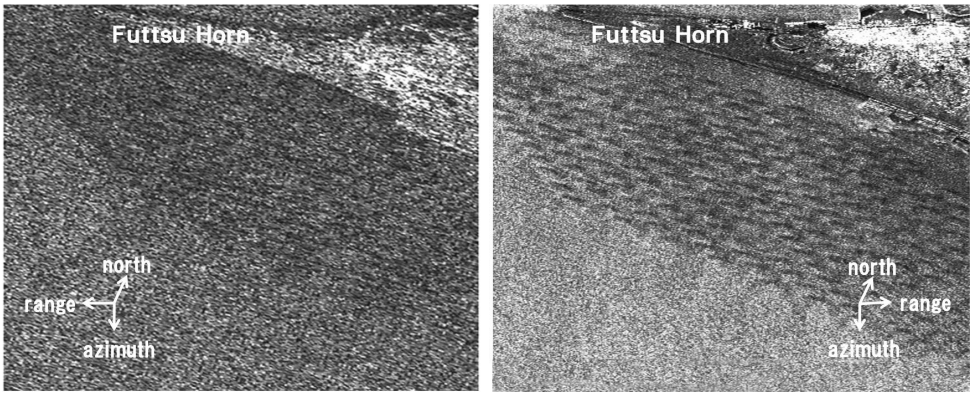

Figure 1: Amplitude image of the laver cultivation area by ALOS-PALSAR (left), and that by TerraSAR-X (right).

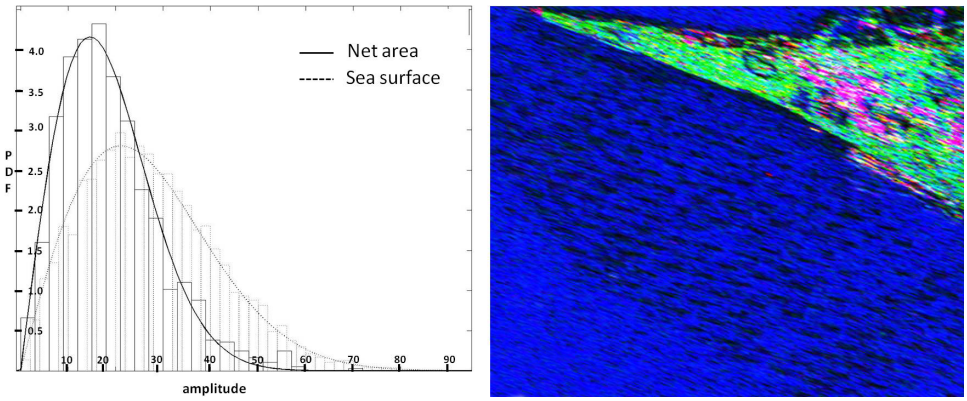

Figure 2: PDF of image amplitude corresponding to the sea surfaces with and without underwater nets (left), and the result of decomposition analysis (right).

surface above the cultivation nets and the relatively bright areas correspond to those without laver nets. From comparison of these images, it is clear that the TerraSAR-X has higher capability of detecting the underwater laver cultivation nets, partly because TerraSAR-X has higher spatial resolution (3.2×3.2 m) than that of PALSAR at PLR-mode (5×23 m in azimuth and slant-range directions respectively). Apart from difference in resolution, there is another reason associated with radar backscatter from surfaces of "effective" roughness at different wavelengths of X-band and the roughness dependence on water depth.

The laver cultivation nets are placed at a few centimeters below the sea surface, so that the small-scale Bragg waves in "shallow water" are damped, resulting in smooth surface in comparison with slightly rough surface in "deep water" without cultivation nets. The RCS from the smooth surface is little for both X-band and L-band, and is almost at a system noise level. The RCS from the slightly rough surface can be sufficiently large at X-band, but this slightly rough surface is effectively smooth at L-band. The difference in RCS between the shallow and deep waters is, thus, small for PALSAR image as compared with TerraSAR-X image.

In oder to prove that RCS from the sea surface above the underwater laver nets is at the noise level, we plotted probability density function (PDF) of each image areas, and carried out the 4-component scattering decomposition analysis [2] using PALSAR PLR data. The left side of Fig.2 is the PDF of amplitude images corresponding to the sea surfaces with and without laver nets (100×100 pixels of each areas). The PDF corresponding to the deep water follows Weibull distribution which is known to describe the radar backscatter from sea surfaces; while the PDF of the cultivation nets obeys Rayleigh distribution which is also well-known to describe Gaussian speckle. Gaussian speckle may be caused by backscatter from a statistically uniform random rough surface or a system noise.

The right image of Fig.2 shows the result of decomposition analysis, where the red, green and blue

colors indicate respectively the surface (single-bounce), volume and double-bounce scattering powers. This result appropriately describes the volume scattering from forested and vegetation areas on land, double-bounce between ground and buildings, and single-bounce from sea surface. However, the net areas are unclassified as black, indicating almost no backscattered power. From these results, we can conclude that little radar backscatter from the sea surface above the underwater laver nets, and the image is composed only of system noise.

3 Polarimetric entropy of PALSAR data

Having shown the difference in scattering mechanisms from the sea surfaces with and without underwater cultivation nets, the analysis based on polarimetric entropy may be considered as the next step [3], since the entropy can describe how dominant the individual scattering processes are. The entropy H is computed using the eigenvalues of covariance matrix or coherency matrix derived from the scattering matrix, defined as

$$H = -\sum_{i=1}^{3} P_i \times \log_3(P_i)\ ;\ P_i = \lambda_i / \sum_{j=1}^{3} \lambda_j \tag{1}$$

for backscatter, where λ_i is the eigenvalue ($\lambda_1 \geq \lambda_2 \geq \lambda_3$), and P_i is the probability that the ith scattering occurs. The range of entropy is $0 \leq H \leq 1$. For example, if $H = 0$, only one eigenvalue exists, implying a single scattering contribution to backscatter, *i.e.*, surface scattering. If $H = 1$, there exist three scattering mechanisms of equal contribution, implying that the scattering process is a random noise process. Then, the entropy of the sea surface with underwater cultivation nets should be higher than the surface without nets, because the former surface is almost specular and the image is a random noise process (system noise); while the surface scattering is dominant in the latter case.

The left image of Fig.3 shows the entropy computed from the PALSAR PLR data. As expected, the entropy of the cultivation area is much larger than the area without nets. Comparison of the entropy image with the amplitude image in the left of Fig.1 shows that the difference of the two areas is enhanced in the entropy image.

For quantitative assessment, the average contrast of the amplitude and entropy in the central part of the underwater net area was computed. The contrast is defined as $C = (\langle A_{max} \rangle - \langle A_{min} \rangle) \,/\, (\langle A_{max} \rangle + \langle A_{min} \rangle)$, where $\langle A_{max} \rangle$ and $\langle A_{min} \rangle$ are respectively the maximum and minimum amplitude or entropy. The result is that $C = 0.122$ for the entropy image, and $C = 0.081$ for the amplitude image.

It then follows that polarimetric entropy can be an effective means of classifying the cultivation and non-cultivation areas. The right of Fig.3 is the PDF of entropy over the the underwater net area indicated by a white rectangle at the top-right and that of open water at the bottom. From the PDF, the threshold

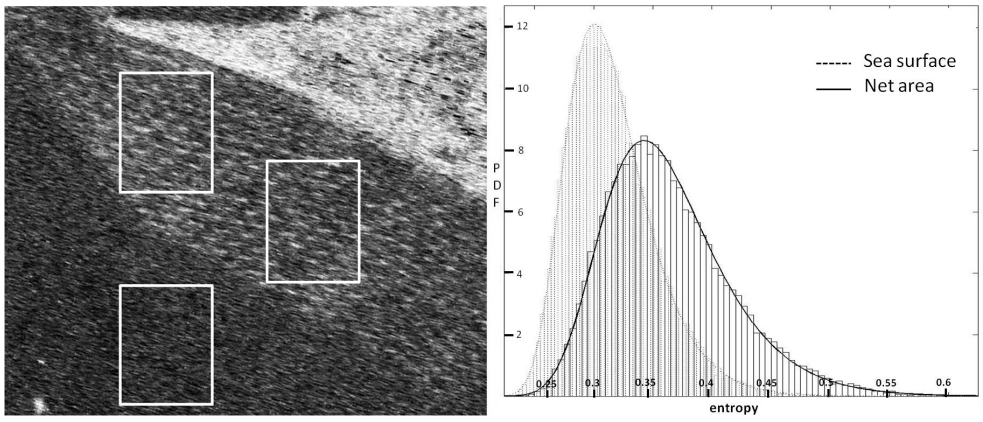

Figure 3: The left is the polarimetric entropy image of ALOS-PALSAR PLR data, and the right is the PDF of the entropy.

value for classification can be considered as the cross-over entropy that is approximately 0.34. Using this threshold value, and the images were classified into two classes. Then, the net area within the white rectangle at the center-right in Fig.3 was estimated from the classified image, and compared with the "ground-truth" data. The result was that the estimated average area per single (combined) net was 3,121 m^2 which is approximately 3 times the true area ($123 \times 8.3 = 1020.9$ m^2).

Since the classification accuracy is not sufficient using the entire pixels within the net area (top-left rectangular in Fig.3), we computed PFD using only the pixels of high entropy corresponding to the net area as shown in the left of Fig.4. The threshold entropy is then found as 0.41. The left of Fig.4 shows the classified entropy image using this threshold value. The estimated area per single net within the white rectangular on the center-right in Fig.3 was 1,211 m^2, and the measurement accuracy was 81%.

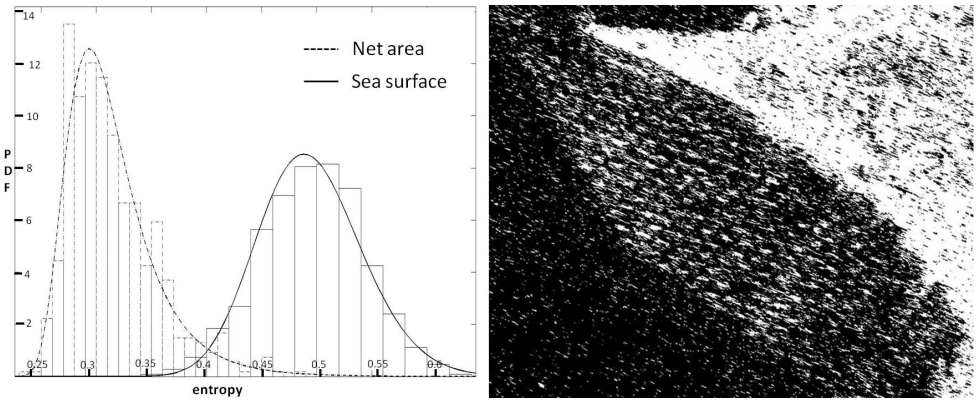

Figure 4: The left is the PDF of entropy over open water (see the left of Fig.3) and selected pixels corresponding to the underwater net area. The right is the classified entropy image with threshold value of $H = 0.41$.

4 Conclusion

In this paper, we described a technique of extracting underwater laver cultivation nets by using entropy analysis from ALOS-PALSAR polarimetric data in the water around the Futtsu Horn, Japan. The cultivation nets were placed a few centimeters below the sea surface, so that the surface, which was effectively in very shallow water, was almost specular under low to moderate wind speeds. A TerraSAR-X amplitude image was also analyzed, showing higher ability of detecting the cultivation nets than PALSAR, because of higher spatial resolution and larger difference in RCS at X-band between the sea surfaces with and without the cultivation nets. This difference in amplitude is too small for PALSAR L-band images to accurately detect the net areas. In order to improve the detection accuracy by PALSAR, we used entropy analysis, resulting in clear difference between the dominant surface scattering of low entropy from open sea surface and the random process (system noise) of high entropy over the underwater net areas. The average accuracy of estimating the cultivation area was found to be approximately 81%. The accuracy under high wind speeds is a subject of future study.

References

[1] NOWPHAS, available from http://www.pari.go.jp/bsh/ky-skb/ks-jyo/kaisy/eng/marine_home_e.htm.

[2] Y. Yamaguchi et. al, "Four-component scattering model for polarimetric SAR image decomposition," IEEE Trans. Geosci. Remote Sens., vol.43, no.8, pp.1699-1706, 2005.

[3] S. R. Cloude and E. Pottier, "An entropy based classification scheme for land applications of polarimetric SAR," IEEE Trans. Geosci. Remote Sens., vol.35, no.1, pp.68-78, 1997.